

Stochastic Thermodynamics of Cooperative Biomolecular Machines: Fluctuation Relations and Hidden Detailed Balance Breaking

D. Evan Piephoff and Jianshu Cao*

Department of Chemistry, Massachusetts Institute of Technology, Cambridge, Massachusetts 02139, United States

We examine a biomolecular machine involving a driven, observable process coupled to a hidden process in a kinetically cooperative manner. A stochastic thermodynamics framework is employed to analyze a fluctuation theorem for the first-passage time of the observable process under nonequilibrium steady-state conditions. Based on a generic kinetic model, we demonstrate that, along first-passage trajectories, entropy production remains constant when the changes in stochastic entropy and free energy of the machine are balanced, which corresponds to zero net hidden flux through the initial state manifold. Under this condition, which we define quite generally, this first-passage time fluctuation theorem can be established, with its violation serving as an experimentally detectable signature of hidden detailed balance breaking (which we subsequently characterize). In addition, using an enzymatic model, we show that the violation of our first-passage time fluctuation theorem can be thought of as a consequence of the breakdown of local detailed balance in the steps linking coarse-grained states that correspond to the initial and intermediate state manifolds. In the absence of hidden current, the fluctuation theorem is restored, and a mesoscopic local detailed balance condition can be established, which has implications for the thermodynamic analysis of driven, coarse-grained systems. This work sheds significant light on the unique connections between stochastic thermodynamic quantities and kinetic measurements in complex cooperative networks.

I. INTRODUCTION

Recent advances in spectroscopic experimental techniques have provided the ability to observe real-time trajectories of biomolecules at the single-molecule level [1, 2]. Such time traces provide insights into microscopic mechanisms that are typically inaccessible from ensemble-averaged measurements [3]. In single-molecule experiments, it is common to measure probability distribution functions (PDFs) of the waiting times between detectable molecular events, such as the first-passage time (i.e., the process completion time) PDF.

Biomolecular machines, including enzymes [4–6] and motor proteins [7–9], consume energy and dissipate heat to perform a given cellular function (e.g., catalysis, cargo transport, etc.). Accordingly, they operate out of equilibrium, frequently in a nonequilibrium steady-state (NESS). In the nonequilibrium scenario, a fluctuation theorem can demonstrate properties of the PDF of a particular thermodynamic quantity (e.g., entropy production) [5]. A time-based fluctuation theorem was recently derived [10, 11] for the first-passage time of entropy production, that is, the time necessary to produce a given amount of entropy. This relation implies equivalence between the normalized forward and backward first-passage time PDFs for entropy production. Based on chemical kinetics, this equivalence—referred to as the generalized Haldane relation—has been demonstrated elsewhere [12, 13] for the forward and backward first-passage time PDFs for a generalized, one-dimensional (1D) enzymatic chain.

In this kinetic chain, the entropy produced along first-passage trajectories is constant. However, for biomolecular machines involving a driven, observable process coupled to a hidden process in a kinetically cooperative [14–18] manner, this is not necessarily the case since such trajectories can start and end in different underlying states; thus, this fluctuation theorem no longer applies for the observable process first-passage time. Moreover, single-molecule spectroscopic experiments have shown that slow, hidden conformational fluctuations can occur on time scales commensurate to those for the observable process [3]; however, many theoretical studies have neglected their role because the calculations involved are quite complex.

We recently analyzed [19] such a first-passage time fluctuation theorem using the canonical model for this type of system, a kinetic scheme for conformation-modulated single-enzyme catalysis under NESS conditions (which has experimental relevance to β -galactosidase [3] and human glucokinase [18]). Our kinetic analysis revealed that in the absence of hidden current, a fluctuation theorem can be established for the observable process first-passage time, and we demonstrated that this dramatic reduction is a general feature applicable to a wide variety of cooperative biomolecular networks. The validity of this expression can be tested experimentally, and its violation serves as a unique signature of hidden detailed balance breaking. In addition, we characterized the deviation from this relation,

* jianshu@mit.edu

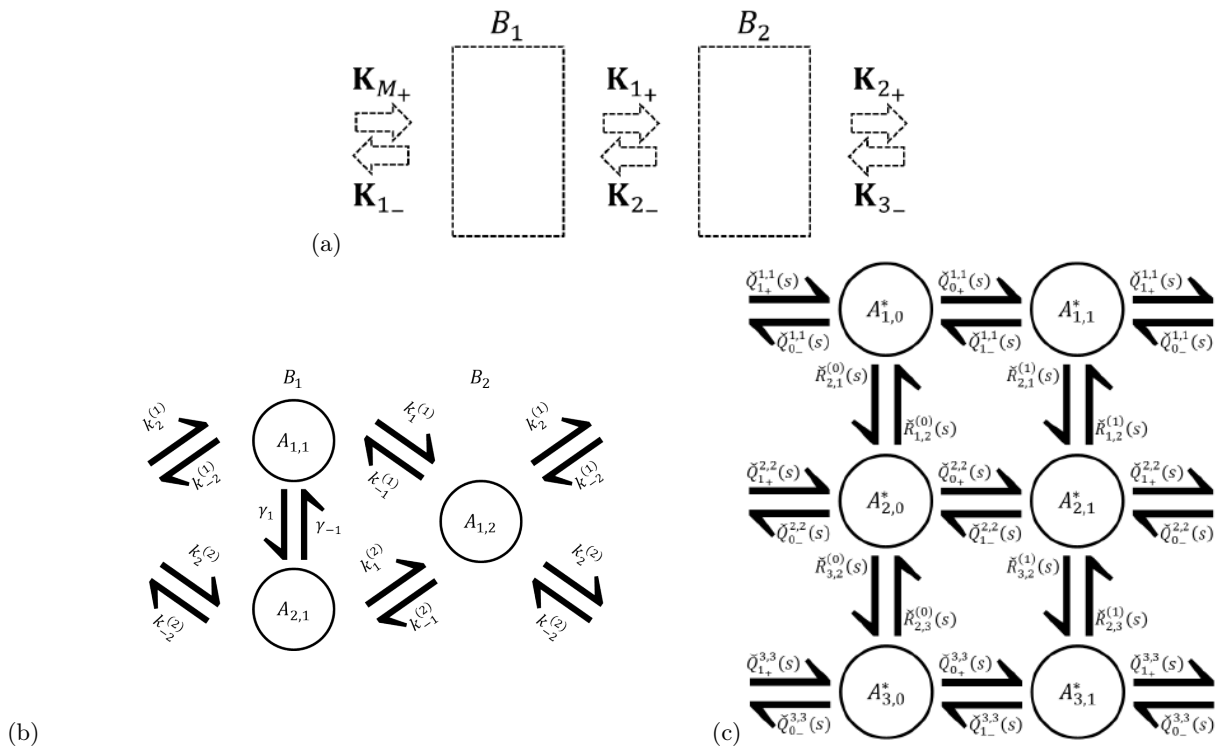


Figure 1. (a) Generic model for a biomolecular machine with kinetic cooperativity under NESS conditions. The machine undergoes a driven, observable, cyclic process cooperatively coupled to a hidden process with dynamics occurring within the state manifolds, $\{B_m\}$, which have largely arbitrary internal topologies and connectivities (see text for details). Transitions between manifolds are designated here as $\{\mathbf{K}_{\pm m}\}$. (b)–(c) Examples of underlying schemes corresponding to the generic kinetic model in (a). The rates of the transitions between the discrete states are represented by $\{k_{\pm m}^{k,l}\}$ and $\{\gamma_{k,l}^{(m)}\}$.

identifying a thermodynamic bound on the kinetic branching ratio (a measure of directionality defined as the ratio of the forward observable process probability to the backward one).

Here, we employ a stochastic thermodynamics framework to interpret our first-passage time fluctuation theorem results [19] and generalize them to a broad class of systems. The key results of this paper are represented in eqs 5–8, 13, and 14. Based on a generic kinetic model for a cooperative biomolecular machine, we demonstrate that, along first-passage trajectories, entropy production remains constant when the changes in stochastic entropy and free energy of the machine are equal, which corresponds to zero net hidden flux through the initial state manifold (i.e., hidden detailed balance). Under this condition, which we define quite generally, our first-passage time fluctuation theorem is restored. Additionally, using an enzymatic model, we show that the violation of this relation can be explained as a consequence of the breakdown of local detailed balance in the steps linking coarse-grained states corresponding to the initial and intermediate state manifolds. In the absence of hidden current, the fluctuation theorem is restored, and a mesoscopic local detailed balance condition can be established, which has implications for the analysis of coarse-grained systems. Lastly, we characterize the deviation from hidden equilibrium by analyzing the kinetic branching ratio for a more complex model, recovering our previously derived thermodynamic bound.

II. GENERIC KINETIC MODEL

We begin by considering the generic model in Figure 1a for a biomolecular machine with kinetic cooperativity [14–17]. Examples of biomolecular machines include molecular motors as well as single enzymes catalyzing the conversion of a substrate to a product. Here, the machine undergoes a driven process (e.g., enzyme turnover) cyclic about (i.e., it begins and ends in) B_1 , the initial state manifold. The overall process is reversible, with both the forward and backward processes traversing the state manifold B_2 . The occurrence of a forward (rightward) B_2 -to- B_1 kinetic manifold transition, directly following a B_1 -to- B_2 forward transition, marks the completion of the forward process, while the occurrence of a backward (leftward) B_2 -to- B_1 manifold transition, directly following a B_1 -to- B_2 backward transition, marks the completion of the backward process. We consider the basic direction of propagation between

state manifolds to be the observable direction of the system, with the corresponding driven process referred to as the observable process.

The observable process is cooperatively coupled to a hidden process (or potentially a set of hidden processes) having dynamics occurring within the manifolds, that of which is the result of simple thermal changes not due to an external driving source (e.g., conformational changes). Each state in B_1 and B_2 has an observable transition entering and exiting it; otherwise, the internal topologies of the manifolds are arbitrary, along with their connectivities. The underlying kinetic scheme (see Figures 1b and 1c for examples) is a network of discrete states with Markovian transition dynamics [20]. The machine is embedded in an aqueous solution that serves as a heat bath with a constant temperature T . Driving sources are taken to be time-independent; therefore, in the long-time limit, the system reaches a NESS.

For our model in Figure 1a, we define a state coordinate x for the machine such that $x \in \mathbb{N}$. The network is described by $A(x)$, where the state of the machine corresponding to $x = i$ is represented as $A(x = i) = A_i$. We can subdivide x into two separate coordinates, x_1 and x_2 , where x_1 corresponds to the hidden direction, and x_2 corresponds to the observable one. Now, the network can be described by $A(x_1, x_2)$, with the state corresponding to $x_1 = l, x_2 = m$ represented as $A(x_1 = l, x_2 = m) = A_{l,m}$. We can envisage the scheme as a network of manifolds described by $B(x_2)$, where the manifold of states corresponding to $x_2 = m$ is represented as $B(x_2 = m) = B_m$. The rate of the hidden transition from $A_{l,m}$ to $A_{k,m}$ is represented as $\gamma_{k,l}^{(m)}$; the rate of the forward (backward) observable transition from $A_{l,1}$ to $A_{k,2}$ ($A_{l,2}$ to $A_{k,1}$) is $k_1^{k,l}$ ($k_{-1}^{k,l}$); and the rate of the forward (backward) periodic observable transition from $A_{l,2}$ to $A_{k,1}$ ($A_{l,1}$ to $A_{k,2}$) is $k_2^{k,l}$ ($k_{-2}^{k,l}$).

A trajectory of duration t is represented as $x(t)$. Changes along $x(t)$ are defined as proceeding from $t = 0$ to t , with the total entropy production along it represented by $\Delta S^{\text{tot}}[x(t)]$. We define τ_{\pm} as the forward/backward first-passage time for the observable process, i.e., the time necessary to complete an iteration of the forward/backward process, while avoiding the completion of the backward/forward one. An individual trajectory corresponding to such an iteration is referred to as a forward/backward first-passage trajectory and is designated as $x_{\pm}(\tau_{\pm})$. The work applied along such a trajectory, $\pm w$, which may include chemical work (see Section III for an explanation), is referred to as the forward/backward first-passage work, with $\Delta s^{\text{tot}} = w/T$. That is, we define Δs^{tot} as the entropy production associated with the first-passage work. The unnormalized PDF of τ_{\pm} is represented as $P_{\pm}(\tau_{\pm})$. When all forward/backward first-passage trajectories produce entropy $\pm \Delta s^{\text{tot}}$, we can write a fluctuation theorem for τ_{\pm} that relates the ratio $P_{+}(t)/P_{-}(t)$ exponentially to Δs^{tot} [10–12], which we refer to as the first-passage time fluctuation theorem (see eq 8 below). However, in a kinetically cooperative biomolecular machine, the entropy produced along first-passage trajectories is no longer constant, since they may begin and end in different underlying states (as shown in Figure 2b below), resulting in a breakdown of this relation. In order to analyze this first-passage time fluctuation theorem in the context of our generic model in Figure 1a, we will employ a stochastic thermodynamics framework to examine $\Delta S^{\text{tot}}[x_{\pm}(\tau_{\pm})]$.

III. ENTROPY PRODUCTION ALONG FLUCTUATING TRAJECTORIES

Here, we make some basic definitions for thermodynamic quantities as they pertain to the system described above. We can write an entropy balance along $x(t)$ as $\Delta S^{\text{tot}}[x(t)] = \Delta S^{\text{sto}}[x(t)] + \Delta S^{\text{mach}}[x(t)] + \Delta S^{\text{med}}[x(t)]$, with the entropy change of the surrounding medium given by $\Delta S^{\text{med}}[x(t)] = -Q[x(t)]/T$, where $-Q[x(t)]$ is the dissipated heat. For convenience, we have incorporated the entropic contribution of the solution into $Q[x(t)]$ (see ref [5] for further details). The change in stochastic entropy of the system along $x(t)$ is expressed as

$$\Delta S^{\text{sto}}[x(t)] = -k_{\text{B}} \ln \left(\frac{\rho^{\text{s}}[x(t)]}{\rho^{\text{s}}[x(0)]} \right) \quad (1)$$

where $\rho^{\text{s}}(x)$ is the stationary population distribution, with $\rho^{\text{s}}(x = i) = \rho_i^{\text{s}}$, and k_{B} is the Boltzmann constant. The energy of A_i is represented as E_i^{mach} , with corresponding intrinsic entropy S_i^{mach} and free energy $F_i^{\text{mach}} = E_i^{\text{mach}} - TS_i^{\text{mach}}$ [21]. We can write a first law-like energy balance along $x(t)$ as $Q[x(t)] + W[x(t)] = \Delta E^{\text{mach}}[x(t)] = \Delta F^{\text{mach}}[x(t)] + T\Delta S^{\text{mach}}[x(t)]$, where $W[x(t)]$ is the work applied to the machine (in the observable direction). In accordance with our above definition of heat, $W[x(t)]$ may include chemical work, i.e., the negative of the free energy change of the solution due to a reaction with stoichiometrically differing total chemical potentials between the reactants and products [5] (example in Section V below). In our system, $W[x_{\pm}(\tau_{\pm})] = \pm w$; that is, the forward/backward first-passage work is path-independent. The entropy balance above can then be rewritten as

$$\Delta S^{\text{tot}}[x(t)] = \Delta S^{\text{sto}}[x(t)] + (W[x(t)] - \Delta F^{\text{mach}}[x(t)])/T \quad (2)$$

We now connect ΔF^{mach} and W to the rates of individual transitions, such as those in the examples depicted in Figures 1b and 1c. We define a discrete transition coordinate z , where the free energy change and applied work associated with the transition corresponding to $z = \xi$ are represented as $\Delta F^{\text{mach}}(z = \xi) = \Delta_\xi F^{\text{mach}}$ and $W(z = \xi) = W_\xi$, respectively. It is noted that an individual transition (in the observable direction) can involve multiple types of work (e.g., chemical, mechanical, etc.), such that $W_\xi = \sum_\eta W_{\xi\eta}$, where the η subscript corresponds to a particular type of work [22]. The coordinate $z_{x(t)}(\tau_j)$ corresponds to the transition completed at τ_j , the time at which the j -th transition (which may or may not be a repeated transition) is completed along $x(t)$. Along such a trajectory, $\Delta F^{\text{mach}}[x(t)] = \sum_j \Delta F^{\text{mach}}[z_{x(t)}(\tau_j)]$ and $W[x(t)] = \sum_j W[z_{x(t)}(\tau_j)]$. For observable transition λ with rate k_λ and hidden transition μ with rate γ_μ , local detailed balance [4, 5] requires that

$$\frac{k_\lambda}{k_{\lambda^\dagger}} = \exp[-\beta(\Delta_\lambda F^{\text{mach}} - W_\lambda)] \quad (3)$$

$$\frac{\gamma_\mu}{\gamma_{\mu^\dagger}} = \exp[-\beta\Delta_\mu F^{\text{mach}}] \quad (4)$$

where the \dagger superscript denotes the reverse transition, with $\Delta_{\xi^\dagger} F^{\text{mach}} = -\Delta_\xi F^{\text{mach}}$ and $W_{\lambda^\dagger} = -W_\lambda$; $\beta = [k_B T]^{-1}$.

IV. ANALYSIS OF FIRST-PASSAGE TRAJECTORIES

Now, we examine entropy production for the generic model in Figure 1a. Here, forward/backward first-passage trajectories that begin and end in the same underlying state (within B_1) produce entropy $\pm\Delta s^{\text{tot}}$. However, because such trajectories can begin and end in different states (as shown in Figure 2b below), $\Delta S^{\text{tot}}[x_\pm(\tau_\pm)]$ is not necessarily constant, as $\Delta S^{\text{sto}}[x_\pm(\tau_\pm)]$ and $\Delta F^{\text{mach}}[x_\pm(\tau_\pm)]$ can be nonzero. In order to achieve $\Delta S^{\text{tot}}[x_\pm(\tau_\pm)] = \pm\Delta s^{\text{tot}}$, it is required that (see eq 2)

$$\Delta S^{\text{sto}}[x_\pm(\tau_\pm)] = \Delta F^{\text{mach}}[x_\pm(\tau_\pm)]/T \quad (5)$$

i.e., that the changes in stochastic entropy and free energy of the machine be balanced along first-passage trajectories. The $A_{l,m}$ stationary population is represented as $\rho^s(x_1 = l, x_2 = m) = \rho_{l,m}^s$. From eqs 1, 3, and 4, we find that eq 5 is satisfied under the hidden detailed balance condition,

$$\frac{\rho_{k,1}^s}{\rho_{l,1}^s} = \frac{\gamma_{k,l}^{(1)}}{\gamma_{l,k}^{(1)}} \quad \forall k, l \quad (6)$$

which corresponds to

$$J_{k,l} = 0 \quad \forall k, l \quad (7)$$

where the stationary hidden population flux from $A_{l,1}$ to $A_{k,1}$ is given by $J_{k,l} = \gamma_{k,l}^{(1)}\rho_{l,1}^s - \gamma_{l,k}^{(1)}\rho_{k,1}^s$. It is noted that the constraints of local detailed balance (eqs 3 and 4) alone are generally insufficient in satisfying hidden detailed balance, as demonstrated in eqs 9–11 below. Equation 6 is a stricter condition than eqs 3 and 4, and it corresponds to zero net hidden flux (i.e., current) through the initial state manifold.

Under eq 6, all forward/backward first-passage trajectories now produce entropy $\pm\Delta s^{\text{tot}}$, so for the generic model in Figure 1a, we can write the first-passage time fluctuation theorem [23] (consistent with our previously reported kinetic analysis [19])

$$\frac{P_+(t)}{P_-(t)} = \exp\left[\frac{\Delta s^{\text{tot}}}{k_B}\right] \quad (8)$$

recovering the form obtained elsewhere for a 1D kinetic chain [12]. That is, in the absence of hidden current, $P_+(t)/P_-(t)$ dramatically reduces to a fluctuation theorem equivalent to the one derived by Roldán and Neri et

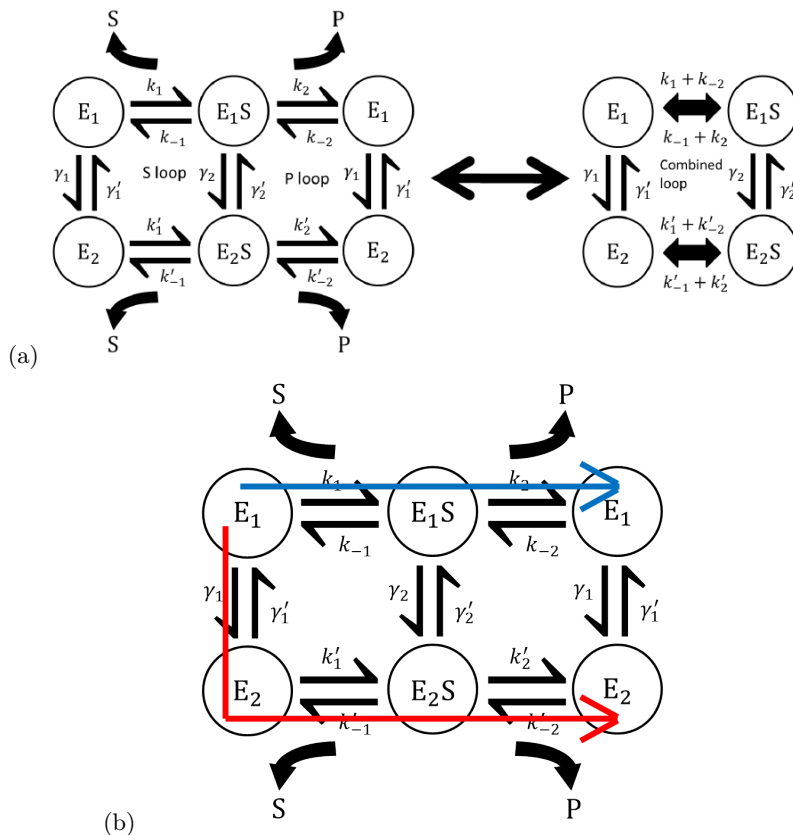


Figure 2. (a) Adaptation of the generic kinetic model in Figure 1a to single-enzyme turnover with conformational interconversion. The enzyme reversibly catalyzes the conversion of a substrate to a product (see text for details). The reaction is cooperatively coupled to a hidden process, with the enzyme undergoing slow conformational changes within B_1 (state manifold for the free enzyme) and B_2 (state manifold for the substrate-bound enzymatic complex). The right-hand side is a representation of the scheme wherein the two steps in each reaction pathway are folded onto each other, resulting in a conformational loop with a corresponding population current J . (b) Depiction of two first-passage trajectories for the model in (a), each producing a different amount of entropy, with the blue one starting and ending in the same underlying state, and the red one doing so in different states.

al. [10, 11] for the first-passage time of entropy production. This result is surprising because, under eq 6, $P_{\pm}(t)$ does not generally reduce to the 1D chain form, but the ratio $P_+(t)/P_-(t)$ does, indicating a unique reduction in how the forward and backward observable processes relate to each another. The normalized PDF corresponding to $P_{\pm}(t)$ is given by $\phi_{\pm}(t) = P_{\pm}(t)/p_{\pm}$, with forward/backward observable process probability $p_{\pm} = \int_0^{\infty} dt P_{\pm}(t)$, where $p_+ + p_- = 1$. Equation 8 implies the symmetry relation $\phi_+(t) = \phi_-(t)$, which is referred to as the generalized Haldane relation and has been derived for a 1D enzymatic chain reaction [12, 13]. Similarly, it was shown that for a 1D kinetic chain involving a motor protein, the mean forward and backward first-passage times are equal [24]. The PDF $\phi_{\pm}(t)$ can be experimentally measured; therefore, the generalized Haldane relation can be tested, and its violation—which implies a violation of the first-passage time fluctuation theorem (eq 8)—serves as a unique signature of hidden detailed balance breaking. It is noted that $P_{\pm}(t)$ (as well as w) can typically also be measured; thus, the first-passage time fluctuation theorem can be directly tested itself. We recently proved this signature using a novel technique to analyze the kinetics; the analysis presented herein interprets this result through the lens of stochastic thermodynamics and generalizes it to a broad class of driven processes with coupled, hidden dynamics.

V. APPLICATION TO SINGLE-ENZYME CATALYSIS

To demonstrate the above results with an illustrative example, we now adapt the generic kinetic model in Figure 1a to an enzymatic reaction with conformational interconversion (shown in Figure 2a). Here, a single enzyme reversibly catalyzes the conversion of a substrate, S , to a product, P . The free enzyme, E (state manifold represented by B_1), can reversibly bind the substrate, resulting in the formation of the substrate-bound enzymatic complex, ES (state

manifold represented by B_2), which can then reversibly undergo product formation. Substrate is consumed to form product in the forward observable process, and product is consumed to form substrate in the backward one. The single enzyme is embedded in a solution of substrate and product, such that the substrate and product concentrations (and chemical potentials) remain fixed here, and the nonlinear substrate binding and reverse product formation kinetic transitions are treated as pseudolinear. The reaction is cooperatively coupled to a hidden process, as the enzyme undergoes slow conformational changes within B_1 and B_2 . Such conformation-modulated enzymatic models have experimental relevance to β -galactosidase [3] and human glucokinase [18]. For convenience, our notation has been modified here, such that the $A_{l,1}$ -to- $A_{l,2}$ ($A_{l,2}$ -to- $A_{l,1}$) transition rates are now represented as $k_1^{(l)}$ and $k_{-2}^{(l)}$ ($k_2^{(l)}$ and $k_{-1}^{(l)}$), and the $A_{1,m}$ -to- $A_{2,m}$ ($A_{2,m}$ -to- $A_{1,m}$) transition rate is now represented as $\gamma_1^{(m)}$ ($\gamma_{-1}^{(m)}$).

Let μ^S represent the chemical potential of the substrate, and μ^P represent that of the product. The reaction process is driven by the difference in chemical potential between the substrate and product (i.e., the chemical affinity), $-\Delta\mu$, that is, $w = \mu^S - \mu^P \equiv -\Delta\mu$. From eqs 3 and 4, it is seen that local detailed balance constrains the transition rates here as [25]

$$\frac{k_1^{(1)}k_2^{(1)}}{k_{-1}^{(1)}k_{-2}^{(1)}} = \frac{k_1^{(2)}k_2^{(2)}}{k_{-1}^{(2)}k_{-2}^{(2)}} = \exp[-\beta\Delta\mu] \quad (9)$$

$$\frac{\gamma_1^{(1)}k_1^{(2)}\gamma_{-1}^{(2)}k_{-1}^{(1)}}{\gamma_{-1}^{(1)}k_{-1}^{(2)}\gamma_1^{(2)}k_1^{(1)}} = 1 \quad (10)$$

Therefore, the kinetics are described by ten independent rates. The hidden (conformational) population current (depicted on the right-hand side of Figure 2a) is given by $J = J_{2,1} = \rho_{1,1}^s \gamma_1^{(1)} - \rho_{2,1}^s \gamma_{-1}^{(1)}$. In addition, $J/\gamma^{(1)} \propto \left[\gamma_1^{(1)} u_1^{(2)} \gamma_{-1}^{(2)} u_{-1}^{(1)} / \left(\gamma_{-1}^{(1)} u_{-1}^{(2)} \gamma_1^{(2)} u_1^{(1)} \right) - 1 \right]$, where $u_{\pm 1}^{(l)} = k_{\pm 1}^{(l)} + k_{\mp 2}^{(l)}$, and $\gamma^{(1)}$ is a scale given by $\gamma^{(1)} = \gamma_1^{(1)} + \gamma_{-1}^{(1)}$. The hidden (conformational) detailed balance condition, under which $J = 0$, can then be expressed here as

$$\frac{\gamma_1^{(1)} u_1^{(2)} \gamma_{-1}^{(2)} u_{-1}^{(1)}}{\gamma_{-1}^{(1)} u_{-1}^{(2)} \gamma_1^{(2)} u_1^{(1)}} = 1 \quad (11)$$

From eqs 9–11, we see that local detailed balance alone is insufficient in satisfying hidden detailed balance. If the two steps in each reaction pathway were folded onto each other (as shown on the right-hand side of Figure 2a), then the satisfaction of hidden detailed balance would correspond to the probability of traversing the resulting loop being directionally invariant. When hidden detailed balance (eq 11) is satisfied here, we can write the first-passage time fluctuation theorem (consistent with our previously reported kinetic analysis)

$$\frac{P_+(t)}{P_-(t)} = \exp[-\beta\Delta\mu] \quad (12)$$

which implies the generalized Haldane relation (see Section IV). The validity of eq 12 can be experimentally tested, with its violation serving as a unique signature of hidden detailed balance breaking.

VI. COARSE-GRAINING AND MESOSCOPIC LOCAL DETAILED BALANCE

In the absence of slow hidden (i.e., conformational) dynamics, the enzymatic model in Figure 2a is described by a 1D kinetic chain with rates $\{k_{\pm m}\}$. In this picture, the rates for each step obey local detailed balance, as they are related by eq 3. As a result, it can be readily shown in this case that [12] $P_+(t)/P_-(t) = k_1 k_2 / (k_{-1} k_{-2}) = \exp[\beta w]$.

In the presence of slow hidden dynamics (i.e., for the model in Figure 2a), the observable (i.e., chemical) states are described by the manifolds $\{B_m\}$. The manifold B_m can be coarse-grained, such that the coarse-grained state \bar{B}_m represents the corresponding hidden (i.e., conformational) ensemble-averaged observable state with stationary population $\bar{\rho}_m^s = \sum_l \rho_{l,m}^s$. As a result of the coarse-graining, local detailed balance breaks down in the steps linking \bar{B}_1 and \bar{B}_2 (i.e., mesoscopic local detailed balance cannot be established). That is, for observable step m with underlying rates $\left\{ k_{\pm m}^{(l)} \right\}_l$, it is found that, in general, $\langle k_m \rangle / \langle k_{-m} \rangle \neq \langle \exp[-\beta(\Delta_m F^{\text{enz}} - W_m)] \rangle$, where the corresponding

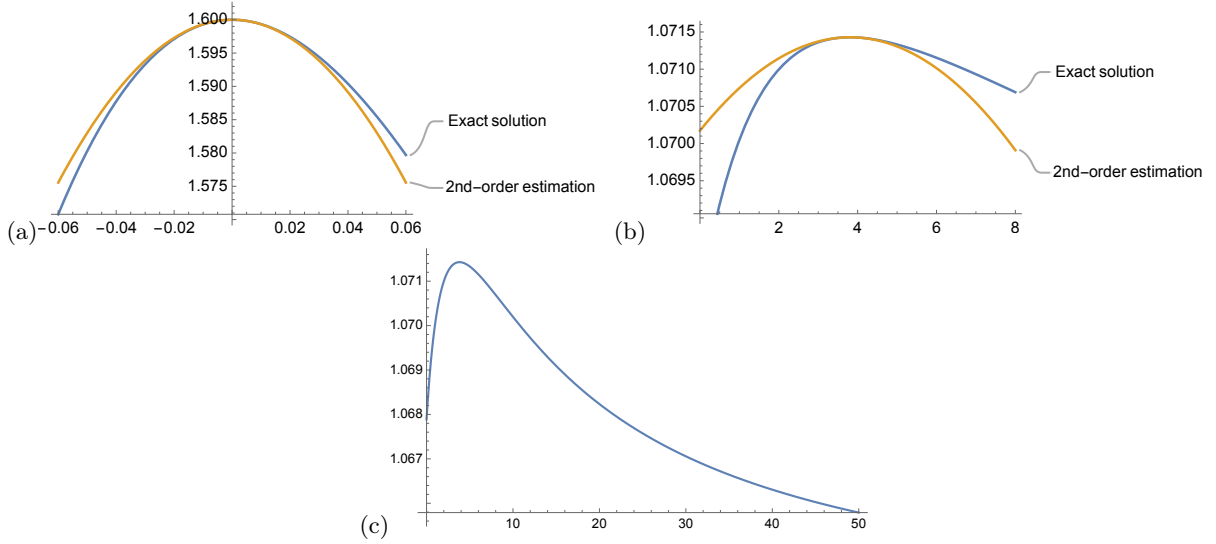


Figure 3. Plots of p_+/p_- against J (a) and $\gamma_1^{(1)}$ (b) and (c) for the model in Figure 2a (see text for details). In (a) and (b), the second-order estimation and the exact solution are shown; (c) shows the full range of the exact solution in (b). In all panels, since $w > 0$, it is seen that the bound $p_+/p_- \leq \exp[\beta w]$ is obeyed.

average forward rate is given by $\langle k_m \rangle = \sum_l \rho_{l,m}^s k_m^{(l)} / \bar{\rho}_m^s$, with $\langle \exp[-\beta(\Delta_m F^{\text{enz}} - W_m)] \rangle = \sum_l \rho_{l,m}^s (k_m^{(l)} / k_{-m}^{(l)}) / \bar{\rho}_m^s$, and the average backward rates are given by $\langle k_{-1} \rangle = \sum_l \rho_{l,2}^s k_{-1}^{(l)} / \bar{\rho}_2^s$ and $\langle k_{-2} \rangle = \sum_l \rho_{l,1}^s k_{-2}^{(l)} / \bar{\rho}_1^s$. Accordingly, $P_+(t)/P_-(t) \neq \langle k_1 \rangle \langle k_2 \rangle / (\langle k_{-1} \rangle \langle k_{-2} \rangle)$ here as well. However, when hidden detailed balance is satisfied, local detailed balance is restored in the steps linking \bar{B}_1 and \bar{B}_2 . That is, under eq 11, for observable step m , we can establish the mesoscopic local detailed balance condition (derivations in the Supporting Information),

$$\frac{\langle k_m \rangle}{\langle k_{-m} \rangle} = \langle \exp[-\beta(\Delta_m F^{\text{enz}} - W_m)] \rangle \quad (13)$$

and we find that

$$\frac{P_+(t)}{P_-(t)} = \frac{\langle k_1 \rangle \langle k_2 \rangle}{\langle k_{-1} \rangle \langle k_{-2} \rangle} = \exp[\beta w] \quad (14)$$

recovering eq 12. Thus, for this model, the violation of the first-passage time fluctuation theorem can be thought of as a consequence of the breakdown of local detailed balance in the steps linking \bar{B}_1 and \bar{B}_2 , that of which is restored in the absence of hidden current. The concept of mesoscopic local detailed balance and its connection to coarse-grained systems will be explored further in a future publication.

VII. HIDDEN DETAILED BALANCE BREAKING

Now, we characterize hidden detailed balance breaking for the four-state model in Figure 2a. We define p_+/p_- as the kinetic branching ratio for the observable process, which serves as a measure of the deviation from hidden equilibrium and is obtainable from experimental measurements. For $J \rightarrow 0$ (i.e., near hidden equilibrium), a second-order expansion of $\frac{p_+}{p_-}(J)$ about $J = 0$ can be written as (see Supporting Information for further details)

$$\frac{p_+}{p_-}(J) \approx \exp[\beta w] + aJ^2 \quad (15)$$

where $a = \frac{1}{2} \frac{d^2}{dJ^2} \left[\frac{p_+}{p_-}(J) \right]_{J=0}$. For $w > 0$ (< 0), $a < 0$ (> 0), i.e., the second-order estimation of $\frac{p_+}{p_-}(J)$ has negative (positive) concavity, consistent with the previously derived inequality $p_+/p_- \leq \exp[\beta w]$ ($\geq \exp[\beta w]$).

Substituting in the local detailed balance constraints (eqs 9 and 10) with $\gamma_1^{(1)}$ and $k_{-2}^{(1)}$, and substituting in J with $k_2^{(1)}$ (these substitution choices are arbitrary), we obtain $\exp[\beta w] = k_1^{(2)} k_2^{(2)} / (k_{-1}^{(2)} k_{-2}^{(2)})$, along with

$$\begin{aligned}
aD = & \left(\gamma_{-1}^{(1)} \gamma_{-1}^{(2)} k_{-1}^{(1)} + \gamma_{-1}^{(1)} \gamma_1^{(2)} k_{-1}^{(2)} + \gamma_{-1}^{(1)} k_{-1}^{(1)} k_{-1}^{(2)} + \gamma_{-1}^{(2)} k_{-1}^{(1)} k_1^{(2)} + \gamma_{-1}^{(2)} k_{-1}^{(1)} k_{-2}^{(2)} + \gamma_{-1}^{(1)} k_{-1}^{(1)} k_2^{(2)} \right) \\
& \times \left(\gamma_1^{(2)} k_{-1}^{(2)2} k_1^{(1)} + \gamma_{-1}^{(2)} k_{-1}^{(1)} k_{-1}^{(2)} k_1^{(2)} + \gamma_{-1}^{(2)} k_{-1}^{(2)} k_1^{(1)} k_1^{(2)} + \gamma_1^{(2)} k_{-1}^{(2)} k_1^{(1)} k_1^{(2)} \right) \\
& + \gamma_{-1}^{(2)} k_{-1}^{(2)} k_1^{(1)} k_{-2}^{(2)} + \gamma_1^{(2)} k_{-1}^{(2)} k_1^{(1)} k_{-2}^{(2)} + \gamma_1^{(2)} k_{-1}^{(2)} k_1^{(1)} k_2^{(2)} + \gamma_{-1}^{(2)} k_{-1}^{(1)} k_1^{(2)} k_2^{(2)} \Big)^2
\end{aligned} \tag{16}$$

where

$$\begin{aligned}
D = & \gamma_{-1}^{(1)2} k_1^{(1)2} k_{-1}^{(2)2} \gamma_1^{(2)} k_{-2}^{(2)} \left(k_{-1}^{(2)} + k_2^{(2)} \right) \left(\gamma_{-1}^{(2)} k_{-1}^{(1)} + \gamma_1^{(2)} k_{-1}^{(2)} \right) \left(\gamma_{-1}^{(2)} k_{-1}^{(1)} + \gamma_1^{(2)} k_{-1}^{(2)} + k_{-1}^{(1)} k_{-1}^{(2)} + k_{-1}^{(1)} k_2^{(2)} \right) \\
& \times \left[k_{-1}^{(2)} k_{-2}^{(2)} / \left(k_1^{(2)} k_2^{(2)} \right) - 1 \right]
\end{aligned} \tag{17}$$

This expansion of $\frac{p_{\pm}}{p_{-}}(J)$, along with the corresponding exact solution, is plotted in Figure 3a, where it is seen that the two match closely for small J . Similarly, for $J \rightarrow 0$, we can expand $\frac{p_{\pm}}{p_{-}}(\gamma_1^{(1)})$ about $\gamma_1^{(1)} = \gamma_{1c}^{(1)}$ —where $\gamma_{1c}^{(1)}$ is the value of $\gamma_1^{(1)}$ that satisfies the hidden detailed balance condition (eq 11)—as $\frac{p_{\pm}}{p_{-}}(\gamma_1^{(1)}) \approx \exp[\beta w] + b \left(\gamma_1^{(1)} - \gamma_{1c}^{(1)} \right)^2$ (see the Supporting Information for further details). Here, $b = \frac{1}{2} \frac{d^2}{d\gamma_1^{(1)2}} \left[\frac{p_{\pm}}{p_{-}}(\gamma_1^{(1)}) \right]_{\gamma_1^{(1)} = \gamma_{1c}^{(1)}}$, with $b < 0$ (> 0) for $w > 0$ (< 0). We plot this expansion of $\frac{p_{\pm}}{p_{-}}(\gamma_1^{(1)})$ in Figure 3b, with the corresponding exact solution shown in Figures 3b and 3c; like before, the two match closely for small J . In all panels of Figure 3, since $w > 0$, it is seen that the bound $p_{+}/p_{-} \leq \exp[\beta w]$ is obeyed.

VIII. CONCLUSIONS

In this paper, we have employed a stochastic thermodynamics framework to interpret our recent kinetic analysis [19] of the first-passage time fluctuation theorem, and to generalize it to a broad class of systems. Based on the generic kinetic model in Figure 1a for a cooperative biomolecular machine, we have demonstrated that, along first-passage trajectories, entropy production remains constant when the changes in stochastic entropy and free energy of the machine are equal, which corresponds to zero net hidden flux through the initial state manifold. Under this condition, which we have defined quite generally, the first-passage time fluctuation theorem is restored, with its violation serving as a detectable signature of hidden detailed balance breaking (which we have also characterized). Additionally, using the enzymatic model in Figure 2a, we have shown that the violation of this relation can be thought of as a consequence of the breakdown of local detailed balance in the steps linking \bar{B}_1 and \bar{B}_2 . In the absence of hidden current, the fluctuation theorem is restored, and a mesoscopic local detailed balance condition can be established, which has implications for the analysis of coarse-grained systems and will be explored further in a future publication.

ACKNOWLEDGMENTS

This work was supported by the NSF (Grant No. CHE-1112825) and the Singapore-MIT Alliance for Research and Technology (SMART). D.E.P. acknowledges support from the NSF Graduate Research Fellowship Program.

-
- [1] W. E. Moerner and D. P. Fromm, Methods of single-molecule fluorescence spectroscopy and microscopy, Rev. Sci. Instrum. **74**, 3597 (2003).
 - [2] H. Park, E. Toprak, and P. R. Selvin, Single-molecule fluorescence to study molecular motors, Q. Rev. Biophys. **40**, 87 (2007).
 - [3] B. P. English, W. Min, A. M. van Oijen, K. T. Lee, G. Luo, H. Sun, B. J. Cherayil, S. C. Kou, and X. S. Xie, Ever-fluctuating single enzyme molecules: Michaelis-Menten equation revisited, Nat. Chem. Biol. **2**, 87 (2006).

- [4] U. Seifert, Stochastic thermodynamics of single enzymes and molecular motors, *Eur. Phys. J. E* **34**, 26 (2011).
- [5] U. Seifert, Stochastic thermodynamics, fluctuation theorems and molecular machines, *Rep. Progr. Phys.* **75**, 126001 (2012).
- [6] Z. Zhang, V. Du, and Z. Lu, Energy landscape design principle for optimal energy harnessing by catalytic molecular machines, *Phys. Rev. E* **107**, L012102 (2023).
- [7] K. Svoboda, P. P. Mitra, and S. M. Block, Fluctuation analysis of motor protein movement and single enzyme kinetics, *Proc. Natl. Acad. Sci. U. S. A.* **91**, 11782 (1994).
- [8] D. Keller and C. Bustamante, The mechanochemistry of molecular motors, *Biophys. J.* **78**, 541 (2000).
- [9] M. P. Leighton and D. A. Sivak, Dynamic and thermodynamic bounds for collective motor-driven transport, *Phys. Rev. Lett.* **129**, 118102 (2022).
- [10] É. Roldán, I. Neri, M. Dörpinghaus, H. Meyr, and F. Jülicher, Decision making in the arrow of time, *Phys. Rev. Lett.* **115**, 250602 (2015).
- [11] I. Neri, É. Roldán, and F. Jülicher, Statistics of infima and stopping times of entropy production and applications to active molecular processes, *Phys. Rev. X* **7**, 011019 (2017).
- [12] H. Qian and X. Sunney Xie, Generalized Haldane equation and fluctuation theorem in the steady-state cycle kinetics of single enzymes, *Phys. Rev. E* **74**, 010902 (2006).
- [13] H. Ge, Waiting cycle times and generalized Haldane equality in the steady-state cycle kinetics of single enzymes, *J. Phys. Chem. B* **112**, 61 (2008).
- [14] A. Fersht, *Enzyme Structure and Mechanism* (W. H. Freeman, New York, 1985).
- [15] J. Cao, Michaelis–Menten equation and detailed balance in enzymatic networks, *J. Phys. Chem. B* **115**, 5493 (2011).
- [16] J. Wu and J. Cao, Generalized Michaelis–Menten equation for conformation-modulated monomeric enzymes, in *Single-Molecule Biophysics: Experiment and Theory*, Advances in Chemical Physics, Vol. 146, edited by T. Komatsuzaki, M. Kawakami, S. Takahashi, H. Yang, and R. J. Silbey (John Wiley & Sons, Inc., Hoboken, 2011) pp. 329–365.
- [17] D. E. Piephoff, J. Wu, and J. Cao, Conformational nonequilibrium enzyme kinetics: Generalized Michaelis–Menten equation, *J. Phys. Chem. Lett.* **8**, 3619 (2017).
- [18] W. Mu, J. Kong, and J. Cao, Understanding the optimal cooperativity of human glucokinase: Kinetic resonance in nonequilibrium conformational fluctuations, *J. Phys. Chem. Lett.* **12**, 2900 (2021).
- [19] D. E. Piephoff and J. Cao, First-passage time fluctuation theorem and thermodynamic bound in cooperative biomolecular networks, arXiv:2501.09087 (2025).
- [20] For thermodynamic consistency, it is required that all kinetic steps be reversible.
- [21] For an extended discussion of intrinsic entropy, we refer readers to Seifert’s work in refs 4 and 5.
- [22] We note that for a mechanically driven system, such as a molecular motor, under a force f with a distance step size d_ξ , $W_\xi = fd_\xi$ (in addition to any chemical or other work contributions).
- [23] Note that the time dependence on the left-hand side of eq 8 divides out.
- [24] A. B. Kolomeisky, E. B. Stukalin, and A. A. Popov, Understanding mechanochemical coupling in kinesins using first-passage-time processes, *Phys. Rev. E* **71**, 031902 (2005).
- [25] It is noted that eq 10 represents the local detailed balance condition for the closed substrate loop. A similar condition can be written for the product loop, $\gamma_1^{(1)}k_{-2}^{(2)}\gamma_{-1}^{(2)}k_2^{(1)} / (\gamma_{-1}^{(1)}k_2^{(2)}\gamma_1^{(2)}k_{-2}^{(1)}) = 1$, which is implied by eqs 9 and 10; however, only two independent constraints can be imposed.